

**MID-HOLOCENE RELATIVE SEA-LEVEL CHANGES ALONG  
ATLANTIC PATAGONIA: NEW DATA FROM CAMARONES,  
CHUBUT, ARGENTINA**

Journal:	<i>The Holocene</i>
Manuscript ID	HOL-16-0133.R2
Manuscript Type:	Paper
Date Submitted by the Author:	n/a
Complete List of Authors:	<p>Bini, Monica; University of Pisa, Earth Dipartimento di Scienze della Terra Isola, Ilaria; Istituto Nazionale Geofisica e Vulcanologia, Sezione Pisa Zanchetta, Giovanni; University of Pisa, Dipartimento di Scienze della Terra Pappalardo, Marta; University of Pisa, Earth Dipartimento di Scienze della Terra</p> <p>Ribolini, Adriano; University of Pisa, Dipartimento di Scienze della Terra Ragaini, Luca; University of Pisa, Dipartimento di Scienze della Terra Baroni, Carlo; Università di Pisa, Dipartimento di Scienze della Terra; Consiglio Nazionale delle Ricerche, Istituto di Geoscienze e Georisorse Boretto, Gabriella; Universidad de Córdoba, Centro de Investigaciones en Ciencias de la Tierra (CICTERRA-UNC)</p> <p>Fuck, Enrique; Universidad Nacional de la Plata</p> <p>Morigi, Caterina; Università degli Studi di Pisa Dipartimento di Scienze della Terra</p> <p>Salvatore, Maria Cristina; Università degli Studi di Pisa Dipartimento di Scienze della Terra</p> <p>Bassi, Davide; Università degli Studi di Ferrara Dipartimento di Fisica e Scienze della Terra</p> <p>Marzaioli, Fabio; Seconda Università degli Studi di Napoli</p> <p>Terrasi, Filippo; 2nd University of Naples, Mathematics and Physics</p>
Keywords:	relative sea level, Atlantic Patagonia, Holocene, coastal geomorphology, Camarones, biological indicators
Abstract:	<p>This paper concerns the relative sea-level changes associated with the Atlantic Patagonian coast derived from sea-level index points whose elevation was determined by a DGPS. Bioencrustations from outcrops located near Camarones, Chubut and Argentina consist of autochthonous deposits characterized by <i>Austrorotalia</i> <i>psittacus</i> MOLINA, 1782, encrusting acervulinid foraminifera, coralline red algae, and bryozoans. The association of the different organisms is interpreted as being associated with an intertidal environment and they have been used as index points to establish the relative sea-level position. The main conclusion was that the relative sea-level between c. 7000 and 5300 cal. yr BP was in the range of c. 4 - 2 m asl, with a mean value of c. 3.5 m asl. Our data seem to support the existence of different rates of relative sea-level fall in different sectors of Atlantic Patagonia during the Holocene, and highlight the importance of</p>

1  
2  
3  
4  
5  
6  
7  
8  
9  
10  
11  
12  
13  
14  
15  
16  
17  
18  
19  
20  
21  
22  
23  
24  
25  
26  
27  
28  
29  
30  
31  
32  
33  
34  
35  
36  
37  
38  
39  
40  
41  
42  
43  
44  
45  
46  
47  
48  
49  
50  
51  
52  
53  
54  
55  
56  
57  
58  
59  
60

	a more precise and accurate relative sea-level estimation by producing new data and revisiting the indicative meaning of most of the indicators so far used in the area.

SCHOLARONE™  
Manuscripts

For Peer Review

1  
2  
3 1  
4 2 MID-HOLOCENE RELATIVE SEA-LEVEL CHANGES ALONG ATLANTIC  
5 PATAGONIA: NEW DATA FROM CAMARONES, CHUBUT, ARGENTINA  
6  
7 3  
8 4  
9

10 5 Bini Monica<sup>1,2</sup>, Isola Ilaria<sup>3</sup>, Zanchetta Giovanni<sup>1,3,4</sup>, Pappalardo Marta<sup>1</sup>, Ribolini  
11 6 Adriano<sup>1</sup>, Ragaini Luca<sup>1</sup>, Baroni Carlo<sup>1,4</sup>, Boretto Gabriella<sup>5</sup>, Fuck Enrique<sup>5</sup>, Morigi  
12 7 Caterina<sup>1</sup>, Salvatore Maria Cristina<sup>1,4</sup>, Bassi Davide<sup>6</sup>, Fabio Marzaioli<sup>7</sup>, Terrasi  
13 8 Filippo<sup>7</sup>  
14  
15  
16  
17  
18 9

19  
20 10 <sup>1</sup> Dipartimento di Scienze della Terra, Via S. Maria 53, 56126 Pisa, Italy

21 11 <sup>2</sup> Istituto Nazionale di Geofisica e Vulcanologia, "Osservatorio Vesuviano", Via Diocleziano, 258,  
22 12 Napoli

23 13 <sup>3</sup> Istituto Nazionale di Geofisica e Vulcanologia, Via della Faggiola 32, 56100, Pisa, Italy

24 14 <sup>4</sup> CNR-IGG, Consiglio Nazionale delle Ricerche, Istituto di Geoscienze e Georisorse, Via Giuseppe  
25 15 Moruzzi 1, 56124, Pisa, Italy

26 16 <sup>5</sup> Facultad de Ciencias Naturales y Museo, Universidad Nacional de La Plata, INGEA, calle 64 n. 3  
27 17 - 1900 La Plata, Argentina.

28 18 <sup>6</sup> Dipartimento di Fisica e Scienze della Terra, Università di Ferrara, via Saragat 1, 44122 Ferrara,  
29 19 Italy

30 20 <sup>7</sup> CIRCE, Department of Mathematics and Physics, Second University of Naples, Caserta, Italy.  
31 21  
32 22

33  
34  
35  
36 23 **Abstract**  
37  
38  
39  
40  
41  
42  
43 24

44  
45 25 This paper concerns the relative sea-level changes associated with the Atlantic Patagonian coast  
46 26 derived from sea-level index points whose elevation was determined by a DGPS. Bioencrustations  
47 27 from outcrops located near Camarones, Chubut and Argentina consist of autochthonous deposits  
48 28 characterized by *Austromegabalanus psittacus* MOLINA, 1782, encrusting acervulinid foraminifera,  
49 29 coralline red algae, and bryozoans. The association of the different organisms is interpreted as being  
50 30 associated with an intertidal environment and they have been used as index points to establish the  
51 31 relative sea-level position. The main conclusion was that the relative sea-level between c. 7000 and  
52  
53  
54  
55  
56  
57  
58  
59  
60

1  
2  
3 32 5300 cal. yr BP was in the range of *c.* 4 - 2 m asl, with a mean value of *c.* 3.5 m asl. Our data seem  
4  
5 33 to support the existence of different rates of relative sea-level fall in different sectors of Atlantic  
6  
7 34 Patagonia during the Holocene, and highlight the importance of a more precise and accurate relative  
8  
9 35 sea-level estimation by producing new data and revisiting the indicative meaning of most of the  
10  
11 36 indicators so far used in the area.  
12  
13  
14 37

### 16 38 **Keywords**

17  
18 39 Relative sea-level, biological markers, Atlantic Patagonia, Holocene  
19  
20  
21 40

### 22 41 **Introduction**

23  
24 42 The impact of sea-level rise is one of the main concerns related to ongoing global warming, and our  
25  
26 43 capacity to estimate the regional-to-local impact on the coast environment relies on the assumption  
27  
28 44 that many local variables are known (e.g., eustatic sea-level component, tectonic uplift,  
29  
30 45 subsidence, glacial isostatic adjustment; Alley et al., 2005; Blum and Roberts, 2009; Milne et al.,  
31  
32 46 2009; PALSEA, 2009; Lambeck et al., 2014). In this framework, the reconstruction of the relative  
33  
34 47 sea-level changes at regional scale during the Holocene is particularly relevant and the accuracy of  
35  
36 48 its estimation is crucial for testing geophysical models (Milne and Mitrovica, 2008).

37  
38  
39 49 With its 2000 km of coast the Atlantic Patagonian passive margin represents a natural link for  
40  
41 50 exploring the relative sea-level evolution between “near” and “far” field sites (Milne et al., 2005;  
42  
43 51 Rostami et al., 2000). Therefore, this is a strategic area in which to focus paleo sea-level studies  
44  
45 52 (Codignotto et al., 1992; Milne et al., 2005; Rutter et al., 1989, 1990; Rostami et al., 2000;  
46  
47 53 Schellmann and Radke, 2000, 2003, 2010; Pedoja et al., 2011; Ribolini et al., 2011; Zanchetta et al.,  
48  
49 54 2014; Isla and Angulo, 2015). However, a precise and accurate estimation of the relative sea-level  
50  
51 55 (RSL) in this area has been complicated by several factors, namely: i) precise and accurate sea-level  
52  
53 56 indicators such as notches, inner terrace margins, coral reefs, and algal encrustations have been  
54  
55 57 rarely used or not found (Pedoja et al., 2011; Ribolini et al., 2011; Bini et al., 2013, 2014); ii) sea-  
56  
57 58  
58 59  
59 60

1  
2  
3 58 level indicators have generally been measured by using a barometric altimeter or graduate bars  
4  
5 59 equipped with spirit level, starting from the local high-tide level implying a wide vertical error up to  
6  
7 60  $\pm 3$  m (Zanchetta et al., 2012, 2014); iii) the coastal area is within the macrotidal regime (Isla and  
8  
9 61 Bujalesky, 2008), and is characterised by high hydrodynamic regimes, so that most of the sea-level  
10  
11 62 indicators are related to surf and storm extension rather than to mean sea-level. As a consequence,  
12  
13 63 Schellmann and Radke (2010) and Zanchetta et al. (2014) reported a different altitudinal estimation  
14  
15 64 for the Holocene RSL, using different indicators related to coastal sediments (i.e., beach ridges,  
16  
17 65 littoral terraces). Some authors take a different approach in measuring reference sea level (e.g. top  
18  
19 66 vs base of beach ridges; Pappalardo et al., 2015), complicating the use of reported data (Codignotto  
20  
21 67 et al., 1992; Rutter et al., 1989, 1990; Pedoja et al., 2011; Ribolini et al., 2011), while others report  
22  
23 68 data related to high-tide level (Schellmann and Radke, 2010 and references therein, Zanchetta et al.,  
24  
25 69 2012, 2014). The correlation between elevation values measured above high tide and values  
26  
27 70 measured above mean sea-level is not so straightforward and regional correlations are complicated.  
28  
29 71 Although the data from this vast region would be of paramount importance, recent geophysical  
30  
31 72 modelling of sea-level change along the South American coast has not accounted for the Patagonian  
32  
33 73 data (Milne et al., 2005), presumably because of their very high level of uncertainty.  
34  
35 74 In this paper we report on a RSL reconstruction based on in situ fossil barnacles and foraminiferal-  
36  
37 75 bryozoan concretions. These sea-level indicators have never been described along the Patagonian  
38  
39 76 coast so far. Here, we describe the indicators found in the territory of Camarones (Chubut,  
40  
41 77 Argentina, Fig.1), one of the nodal areas for the reconstruction of the relative sea-level oscillations  
42  
43 78 along the Patagonian coast owing to its abundance of raised beaches with datable materials  
44  
45 79 (Schellmann and Radke, 2010; Zanchetta et al., 2012; Pappalardo et al., 2015). Moreover, the  
46  
47 80 elevation of the indicators was for the first time measured by a Differential Global Position System  
48  
49 81 (DGPS), which provided reliable sea-level values at an accuracy never previously reached along the  
50  
51 82 Patagonian coast. Finally, we standardized our data in terms of sea-level index and limiting points  
52  
53  
54  
55  
56  
57  
58  
59  
60

1  
2  
3 83 (e.g. Shennan et al., 2015; Vacchi et al., 2016; Rovere et al., 2016 ). This approach, totally new for  
4  
5 84 the Patagonian coast, is mandatory for future regional and extra-regional correlations.  
6

7 85

8  
9  
10 86 **The study area**

11 87

12  
13  
14 88 The study area is located in the southern part of the Bahía Camarones, Chubut (Argentina), a *c.* 40  
15  
16 89 km wide gulf extending from *c.* 44°54' S to 44°34' S (Fig. 1). Structurally, the area is located on the  
17  
18 90 southern edge of the so-called “North Patagonia Massif” (Ferruglio, 1950). Mostly Jurassic volcanic  
19  
20 91 rocks formed the pre-Quaternary succession (Marifill Formation, Lema et al., 2001). Inland  
21  
22 92 morphology is characterised by flat surfaces covered by Late Neogene-Early Quaternary fluvial  
23  
24 93 gravelly deposits (“*rodados Patagónicos*” in Martinez and Coronato, 2008), while the landscape is  
25  
26 94 dominated by Quaternary littoral and continental deposits raised at various elevations close to the  
27  
28 95 coast (Lema et al., 2001; Pappalardo et al., 2015).

29  
30  
31 96 Like most of coastal Patagonia, the area is dominated by high-energy, macro-tidal and stormy  
32  
33 97 conditions (Isla and Bujaleski, 2008), resulting in a coastal morphology dominated by cliffs, shore  
34  
35 98 platforms and coarse-clastic beach ridges (“swash built ridges” *sensu* Tanner, 1995).

36  
37  
38 99 In Camarones the predictions of the astronomic tide elevations are calculated in relation to the  
39  
40 100 harbour of Puerto Santa Elena (Fig. 1) according to the data released by the Servicio de Hidrografia  
41  
42 101 Naval (<http://www.hidro.gov.ar>). For the area of Camarones the maximum tidal range is *c.* 5 m,  
43  
44 102 while the mean is *c.* 3.5 m (Fig. 2).

45  
46  
47 103 Most of the studies on Holocene coastal evolution are concentrated in the southern part of the Bahía  
48  
49 104 Camarones area, and provide a robust chronological constraint for coastal aggradation during the  
50  
51 105 Holocene (Codignotto et al., 1992; Schellmann 1998; Schellmann and Radtke 2000, 2003, 2010).

52  
53  
54 106 Two evolutionary phases have been distinguished: 1) the first phase, the maximum Holocene  
55  
56 107 ingression (*c.* 6.8-6.5 ky BP), is characterized by the formation of littoral and estuarine deposits  
57  
58 108 (Schellmann and Radke, 2010) found at the sea embayment along local creeks (locally named  
59  
60

1  
2  
3 109 “cañadon”); 2) the successive phase, still active, is marked by discontinuous coastal aggradation,  
4  
5 110 with the formation of prominent higher gravelly beach ridges parallel to the present-day coast (Fig.  
6  
7 111 3).  
8

9  
10 112

### 11 113 **Methodology**

12  
13  
14 114

15  
16 115 For stratigraphic and geomorphological investigations we followed the same approach already used  
17  
18 116 in previous studies conducted in the area (Ribolini et al., 2011, Isola et al., 2011). A preliminary  
19  
20 117 remote sensing analysis was performed by using LANDSAT7 images (acquisition dates, 1999-  
21  
22 118 2001), and Quick Bird images (acquisition date, 2004) supported by the digital elevation model  
23  
24 119 SRTM ([www.jpl.nasa.gov/srtm](http://www.jpl.nasa.gov/srtm)). After this preliminary phase, field surveys were carried out in  
25  
26 120 February 2009, 2010, and 2011 (Zanchetta et al., 2012; Pappalardo et al., 2015). In the first phase,  
27  
28 121 the elevation data were obtained by using graduate bars equipped with spirit level, starting the  
29  
30 122 measurements from the nearest IGN point (Instituto Geográfico Nacional), with a precision in the  
31  
32 123 order of  $\pm 0.3$  m (Zanchetta et al., 2014). A field survey conducted in January 2016 was dedicated to  
33  
34 124 the DGPS measurement of sea-level indicators. The data were acquired by the WGS84 Geographic  
35  
36 125 Coordinate System (maximum error in elevation of acquired points was 10 cm) and post-processed  
37  
38 126 and referred to the current global geoid model EGM2008 (Pavlis et al. 2012) (4 cm planimetric  
39  
40 127 error and 9 cm elevation error). Elevation measurements indicated as “asl” in this paper are referred  
41  
42 128 to the vertical datum EGM2008. These data integrate and basically confirm those previously  
43  
44 129 obtained by graduated bar measurement. For the study area Schellmann and Radke (2010) reported  
45  
46 130 the altitudinal measurement of different sea-level indicators, by using a barometric altimeter  
47  
48 131 (reported precision  $\pm 1$  m) daily calibrated with the tide level. In order to compare our data with  
49  
50 132 those reported by Schellmann and Radke (2010) we used the DGPS to re-measure some of the  
51  
52 133 sections described by Schellmann and Radke (2010).  
53  
54  
55  
56  
57  
58  
59  
60

1  
2  
3 134 *In situ* barnacles and encrusting foraminiferal deposits were collected in the field and measured with  
4  
5 135 DGPS (Figs. 1 and 3), alongside additional samples with articulated valves of *Mytilus edulis* from  
6  
7 136 littoral deposits. The samples for radiocarbon dating were cleaned in an ultrasonic bath with the  
8  
9 137 addition of oxygen peroxide and then gently etched with diluted HCl to remove any recent  
10  
11 138 carbonate encrustation. Radiocarbon measurement was carried out at the CIRCE laboratory of  
12  
13 139 Caserta, Italy (Terrasi et al., 2007, 2008) and calibrated by using the Marine13 curve (Reimer et al.,  
14  
15 140 2015). However, the reservoir effect values for the Southern Atlantic Ocean and, in particular,  
16  
17 141 Patagonia, are not well constrained (Schellmann and Radtke, 2010). Specific studies suggest that for  
18  
19 142 different localities of the Patagonian coast between *c.* 42°S and 50°S the reservoir effect can vary  
20  
21 143 between 180 and 530 years (Cordero et al., 2003; Butzin et al., 2005, Schellmann and Radtke,  
22  
23 144 2010).  
24  
25  
26  
27 145 Collected species, radiocarbon dates and sampling site elevation are reported in Table 1. The state  
28  
29 146 of preservation of barnacles and encrustations, **prior to dating were** assessed by stereomicroscope  
30  
31 147 analysis of thin sections and was investigated by X- Ray power Diffraction (XRD).  
32  
33  
34  
35

## 36 149 **Results**

37  
38 150  
39  
40 151 The study area is located along a small river to the south of the Camarones village (Fig. 1). A  
41  
42 152 succession of Holocene-Pleistocene gravelly beach ridges forms the coastal strandplain, up to a  
43  
44 153 distance of more than 500 m inland from the present coastline. This arched beach ridge system is  
45  
46 154 incised by a river valley where alluvial, marsh and coastal sediments were deposited (Figs. 3 and  
47  
48 155 4a). Along the river valley, bedrock crops out forming steep cliffs in some places and relict shore  
49  
50 156 platforms locally. Three rocky outcrops, composed by welded ignimbrites of Marifil Formation,  
51  
52 157 yielded barnacles (*Austromegabalanus psittacus* Molina, 1782) and foraminiferal encrustations  
53  
54 158 (mostly *Acervulina inhaerens* Schulthe, 1854) in life position (Figs. 3, 4b, 4c, 4d, 5 and 6). The first  
55  
56 159 outcrop (Figs. 3 and 4b) is formed by a vertical cliff exposed for *c.* 3-4 m and a flat top surface,  
57  
58  
59  
60



1  
2  
3 160 located at *c.* 5 m asl, representing the remnant of a shore platform. Barnacles and foraminiferal  
4  
5 161 encrustations are located on the cliff where barnacles are discontinuously spread for less than 1 m  
6  
7 162 (between 3.4 m asl and 3.8 m asl) and encrustations for *c.* 1.5 m (between 3.3 m asl and 4.8 m asl;  
8  
9 163 Figs. 4b and 5). The second outcrop (Figs. 3, 4c, and 5) is formed similarly by a vertical cliff with  
10  
11 164 an on-top shore platform covered by gravelly deposits. On the vertical cliff barnacles span between  
12  
13 165 3.1 m and 3.9 m asl and incrustations from 3.3 m and 4.6 m asl. The third sampled inland site is  
14  
15 166 represented by boulders at the toe of a rocky cliff (Figs. 3, 4d and 5). Barnacles and incrustations,  
16  
17 167 spanning in elevation between 3.2 and 4.2 m asl, developed on the blocks and at the base of the  
18  
19 168 cliff.

20  
21  
22  
23 169 In each sampled site barnacles (*A. psittacus*) occur as isolated or 2-3 jointed individuals (Fig. 6).  
24  
25 170 Most of the encrustations consist of foraminifera identifiable as *Acervulina inhaerens* (Fig. 6d, e, f),  
26  
27 171 which is the dominant component, while arborescent forms such as *Homotrema* and *Miniacina* are  
28  
29 172 less frequent. All these encrusting foraminifera form repetitive or randomly-arranged inner  
30  
31 173 superimposed growth stages. Superimposed growth stage bryozoans and rare coralline-red algal  
32  
33 174 thalli occur within the *A. inhaerens*. The bryozoans are represented by encrusting cheilostomes  
34  
35 175 (*Anascina?*), and the very low preservation does not allow their systematic identification. The  
36  
37 176 corallines are almost micritized and/or recrystallized. A possible uniporate conceptacle was also  
38  
39 177 identified. This reproductive character along with the vegetative characters (cell fusions,  
40  
41 178 monomerous cell filaments) suggests a possible ascription to the Mastophoroideae subfamily (Fig.  
42  
43 179 6d, e, f).

44  
45  
46  
47 180 The top surface of the first outcrops is carved in a previously modelled rocky terrace attributed by  
48  
49 181 Schellmann and Radke (2010) to marine isotope stage 7 (MIS 7). A shell accumulation of *M. edulis*  
50  
51 182 rests directly on the lateral margin of the lower shore platform, sealed by a few decimetre-thick  
52  
53 183 slope deposits. No other deposits cover the shore platform. This shell accumulation, with a poor  
54  
55 184 sandy matrix of some mm-size rounded-clasts, and some shells with valves still joined, is consistent  
56  
57 185 with a storm deposit. One shell from the accumulation yielded a radiocarbon age of 5562±43 yr BP.  
58  
59  
60

1  
2  
3 186 Concretion from the vertical cliff of this outcrop yielded a radiocarbon age of  $4995\pm 89$  yr BP,  
4  
5 187 whereas one barnacle yielded  $5515\pm 50$  yr BP.

6  
7 188 The top surface of the second rocky outcrop is covered by gravelly deposits, which did not yield  
8  
9 189 suitable material for dating (i.e., only fragmented shells and not entire shells with articulated  
10  
11 190 valves). However, these deposits are reasonably related to the formation of the Holocene erosional  
12  
13 191 platform. In the vertical cliff of this second outcrop a barnacle yielded a radiocarbon age of  
14  
15 192  $5132\pm 67$  yr BP. Here, the rocky cliff was crossed by some vertical fissures containing sediment and  
16  
17 193 by some fossil remains, including *M. edulis* and barnacles (Fig. 6c). One sample with articulated  
18  
19 194 valves of *M. edulis* collected from the infilling of the vertical fissures yielded a radiocarbon age of  
20  
21 195  $5567\pm 44$  yr BP.

22  
23  
24 196 On the third site a sample of barnacles revealed a radiocarbon age of  $5641\pm 46$  yr BP.

25  
26  
27 197 All the rocky cliffs are partially sealed by gravelly estuarine terraced deposits, namely valley-mouth  
28  
29 198 terraces, according to Schellman and Radke (2010, Fig. 3). These deposits contain shells  
30  
31 199 (principally *Prothotaca antiqua* and *M. edulis*) accumulated in lenses for which Schellman and  
32  
33 200 Radke (2010) reported a radiocarbon age of  $5560\pm 38$  yr BP. A new radiocarbon measurement was  
34  
35 201 undertaken on an *M. edulis* from the same deposits, directly sealing the second cliff, yielding a  
36  
37 202 consistent age of  $5370\pm 60$  yr BP.

38  
39  
40 203

#### 41 42 204 **Discussion**

43  
44  
45 205 Sea-level indicators in Atlantic Patagonia have yielded controversial results in the estimation of past  
46  
47 206 RSL, and their accuracy and precision have been poorly defined, both for the precision of the  
48  
49 207 measurement of the method applied (barometric altimeter, local maps, graduate bars) and for the  
50  
51 208 unclear meaning of the indicators, e.g. storm, maximum high tide (Codignotto et al., 1992).  
52  
53 209 Therefore, it is mandatory to transform sea-level indicators into index or limiting points to improve  
54  
55 210 RSL estimations (Shennan et al., 2015). So far, the most precise and accurate indicators described  
56  
57 211 for Atlantic Patagonia, which can be easily transformed into sea-level index points, are the erosive  
58  
59  
60

1  
2  
3 212 notches. Specifically, the retreat-point of notch defines the main high tide values ( $\pm 0.3$  m, Bini et  
4  
5 213 al., 2014).

6  
7 214 The Camarones association of barnacles, bryozoans and encrusting foraminifera can be generically  
8  
9 215 interpreted as intertidal-subtidal indicator (e.g. Pirazzoli et al., 1985; Laborel and Laberel-Deguen,  
10  
11 216 1994; Baker et al., 2001; Ferranti et al., 2006; Rovere et al., 2015, 2016).

12  
13 217 Specifically, the collected samples of barnacle correspond to the “acorn barnacle” *A. psittacus* (Fig.  
14  
15 218 6a), a species inhabiting mainly rocky substrates of the subtidal zone, where it forms dense  
16  
17 219 aggregates between 5 and 7 m in water depth (López et al., 2010). However, the functional faculties  
18  
19 220 of the barnacle could account for the high capacity of *A. psittacus* to also colonize habitats exposed  
20  
21 221 to prolonged emersion periods like those characterizing intertidal settings (López et al., 2003). The  
22  
23 222 barnacles generally live in groups forming dense hummocks, but in less favorable locations like the  
24  
25 223 intertidal zones where they are less frequent and distant from each other. The relatively sparse  
26  
27 224 association of barnacles in our sampling sites indicates the upper limit of the living range.

28  
29 225 Present-day acervulinid foraminifera show a large bathymetric range from the intertidal zone down  
30  
31 226 to 100 m in water depth (Perry and Hepburn, 2008; Bassi et al., 2012). Although acervulinids are  
32  
33 227 more common in deeper water settings where interspecific competition for space may be reduced  
34  
35 228 (Rasser and Piller, 1997), *Acervulina inharens* thrives in shallow water Bahamas shelf settings (<  
36  
37 229 30 m; Walker et al., 2011). *Homotrema* is reported from high-energy shallow-water settings  
38  
39 230 (Gischler and Möder, 2009). So far, *Homotrema* has seemed to be an excellent indicator of high-  
40  
41 231 energy water conditions for shallow near-shore and shelf/edge habitats, where water energy during  
42  
43 232 tidal exchange is greater in tropical and subtropical environments (Walker et al., 2011) and, even in  
44  
45 233 this case, it is consistent with the intertidal zone. Moreover, it is generally assumed that fossil  
46  
47 234 barnacles and bio-encrustation in growth positions are easily eroded (Pirazzoli et al., 1985).  
48  
49 235 Therefore, the survival of encrusted shell remains at higher-than-present levels suggests a sea-level  
50  
51 236 fall sufficiently rapid for the shell to escape obliteration by wave erosion (Pirazzoli et al., 1985), a  
52  
53 237 condition favoring the preservation of species that live in the upper limit of the high tide. In most  
54  
55  
56  
57  
58  
59  
60

1  
2  
3 238 cases, the age of the outer shells on a thick vertical encrustation will correspond to the terminal  
4  
5 239 period of the former sea-level stand (Baker et al., 2001). Therefore, the Camarones barnacles,  
6  
7 240 bryozoans and encrusting foraminifera association can be considered substantially intertidal and its  
8  
9 241 definition of index point could be possible on the basis of tide oscillations (Shennan et al., 2015;  
10  
11 242 Vacchi et al., 2016). By assuming that our association is strictly intertidal between *c.* 6100 cal yr  
12  
13 243 BP and *c.* 5300 yr cal. BP RSL was around 3.7 and 3.9 m asl (Fig. 7).

14  
15  
16 244 For the studied area, Schellmann and Radke (2010) reported several radiocarbon measurements for  
17  
18 245 different sea-level indicators, which can complete and improve the interpretation of the data  
19  
20 246 discussed in this paper. In our study, we selected only the valley-mouth terrace sea-level indicators,  
21  
22 247 which are less affected by storm deposition, compared to beach-ridges, thus reducing the errors in  
23  
24 248 elevation estimation (Schellmann and Radke, 2010; Tamura, 2012; Zanchetta et al., 2014).  
25  
26 249 According to the observations of modern analogs by Schellmann and Radke (2010), valley-mouth  
27  
28 250 terraces are estuarine deposits that contain lateral/vertical interfingering of mollusc-bearing littoral  
29  
30 251 sediments and fluvial deposits forming at the mouth of small local rivers. The top of the valley-  
31  
32 252 mouth terraces correlates directly to the former elevation of the high-tide level representing a  
33  
34 253 suitable indicator to be used as index point. As can be inferred from Fig. 7, RSL from mouth-  
35  
36 254 terraces is consistent within the indicative meaning of barnacles and encrustations supporting our  
37  
38 255 interpretation. Indeed, at least three of our biological indicators, chronologically overlapping the  
39  
40 256 data from valley mouth-terraces, lie within 1 m of the top of the mouth-terraces. Significantly, the  
41  
42 257 presence of the storm deposit dated *c.* 5950 cal. yr BP, located directly on the erosive shore  
43  
44 258 platform on top of the first cliff, represents an upper RSL limiting point (Fig. 7), constraining fairly  
45  
46 259 well the values of fossil barnacles and mouth-terrace. The storm deposit can also be considered a  
47  
48 260 *terminus ante quem* for the formation of the rock platform on top of the first outcrop.

49  
50  
51 261 Considering the elevation of the index points obtained from mouth-terraces in the area together with  
52  
53 262 the biological indicators discussed in this paper, this evidence collectively (Fig. 7) agrees on  
54  
55 263 indicating the RSL to be from *c.* 2 to *c.* 4 m asl between *c.* 5300 and 7000 cal. yr BP.  
56  
57  
58  
59  
60

1  
2  
3 264 In Fig. 7, the altimetric and chronological data of the valley-mouth terraces show a highstand  
4  
5 265 between *c.* 7000 and 6600 cal. yr BP at *c.* 4 m asl, followed by a progressive fall to *c.* 2-2.5 m  
6  
7 266 between 6200 and 5300 cal. yr BP. The radiocarbon age of the storm deposit above the shore  
8  
9 267 platform may indicate that this shore platform was related to the higher sea stand at *c.* 7000 cal. yr  
10  
11 268 BP, and was no longer significantly active during the progressive fall after ca. 6200 cal. yr BP, only  
12  
13 269 occasionally reached by storms. However, the RLS variation recorded by the valley mouth terraces  
14  
15 270 is not shown by barnacles and encrustation, thus suggesting that most of this variation falls within  
16  
17 271 the range of error of the two index points.

18  
19  
20 272 Following **Shennon** and Horton (2002) the total vertical error (including vertical distribution of  
21  
22 273 encrustation and barnacles, fig. 5; measurement errors and indicative meaning) for the biological  
23  
24 274 sea-level indicators is *c.* 3.8 m. According to Schellman and Radke (2010), a minimum vertical  
25  
26 275 error for valley mouth-terraces can be calculated at *c.* 2 m. However, a precise estimation of error  
27  
28 276 should be associated with an accurate review of modern analogues on the valley mouth-terraces and  
29  
30 277 of other findings from fixed biological indicators.

31  
32  
33  
34 278 Overall, the mean RSL between *c.* 7000 and 5300 cal. yr BP, which can be obtained considering all  
35  
36 279 the index points, is  $3.4 \pm 0.6$  m asl.

37  
38 280 Initial glacio-hydro-isostatic models of the Patagonian coast suggested that the shoreline could be  
39  
40 281 characterized by currently raised beaches, which started to form as soon as ice-sheet melting ceased  
41  
42 282 (Clark et al., 1978). A more recent model (Milne and Mitrovica, 2008) predicted that relative sea-  
43  
44 283 levels might have exceeded present by *c.* 5 m at 6000 cal. yr BP. Field evidence indicates that the  
45  
46 284 highstand is somewhat *c.* 1.5 m lower than model prediction. These ranges of measurement can  
47  
48 285 agree with the model considering all the vertical errors associated with the index points discussed.

49  
50 286 A comparison of the different sectors of the Atlantic Patagonian coast is complicated by many  
51  
52 287 factors. Codignotto et al. (1992) found a significant rate of relative sea-level changes during the  
53  
54 288 Holocene in relation to different tectonic sectors. They indicated a maximum highstand at *c.* 12 m  
55  
56 289 asl for the period *c.* 4-8 kyr BP for the area of Camarones-Bustamante, at *c.* 2 m asl for the period *c.*  
57  
58  
59  
60

1  
2  
3 290 4-6 kyr BP in the area of Bahia Solano (Fig. 8). These data are affected by poor quality radiocarbon  
4  
5 291 dating together with low altimetric accuracy. Moreover, most data are obtained by measuring the  
6  
7 292 altitudinal crest of beach ridges, which are largely affected by storm conditions (Schellmann and  
8  
9 293 Radke, 2010; Tamura, 2012; Zanchetta et al., 2014). On the contrary, Schellmann and Radke (2010)  
10  
11 294 observed no appreciable differences along the Patagonia coast. However, by using different sea-  
12  
13 295 level indicators the authors observed different values (reported above high tide –a.h.T) for the  
14  
15 296 highstand, occurring between *c.* 6-7 cal. kyr BP, ranging from *c.* 9 to 5 m ahT. Bini et al. (2013,  
16  
17 297 2014), and Zanchetta et al. (2014) reported a relative sea-level at *c.* 8 m asl at *c.* 3500 cal. yr BP by  
18  
19 298 accurate measurements of erosive notches in the Puerto Deseado area (Fig. 1). Owing to the  
20  
21 299 difficulty in dating erosive notches, Zanchetta et al. (2014) suggested that these notches were  
22  
23 300 formed during a previous Holocene highstand. In any case, the relative sea-level marked by well-  
24  
25 301 preserved notches is higher than that observed in the Camarones area, indicating that a different  
26  
27 302 relative sea-level may exist along the Patagonian coast during the same period (Fig. 8).  
28  
29  
30  
31 303 In this respect, Pedoja et al. (2011) suggested that the presence of the Nazca and the Antarctic plates  
32  
33 304 subducting under South America and southern Patagonian respectively (Ramos and Ghiglione,  
34  
35 305 2008, and references therein) may have produced a long wavelength tectonic effect, onto which the  
36  
37 306 glacio-hydro-isostatic signal is overprinted. This signal can vary according to the different sectors  
38  
39 307 of the Atlantic Patagonian coast. More recently, Isla and Angulo (2015) in an accurate review of  
40  
41 308 existing data from MIS5 terraces along Atlantic Patagonia have shown the importance of the effect  
42  
43 309 of subducing plates in determining regional trends in the rate of uplift. The data discussed in our  
44  
45 310 paper seem to support the possible existence of a different uplift rate over the Atlantic Patagonian  
46  
47 311 coast. However, subtle differences can only be identified by appropriate markers and are probably  
48  
49 312 difficult to identify by using the data so far available, which are affected by large measurement  
50  
51 313 uncertainty and incomplete understanding of the indicator meaning.  
52  
53  
54  
55  
56  
57  
58  
59  
60

## 315 **Conclusion**

1  
2  
3 316

4  
5 317 We have presented the first accurate Middle Holocene RSL determination for a well-dated period of  
6  
7 318 time by using different sea-level indicators, for the Atlantic Patagonian coast, with altitudinal  
8  
9 319 measurement obtained using DGPS. Once dated, and their meaning and vertical error discussed, the  
10  
11 320 indicators were transformed into index points. In this paper, using the available evidences, we  
12  
13 321 suggest that the *in situ* association of sparse barnacles, bryozoans and encrusting foraminifera can  
14  
15 322 have the indicative meaning of intertidal indicators, in the absence of modern analogs for the area.  
16  
17 323 The mean RSL was estimated at c. 3.50 m asl, lower than the c. 5 m predicted by the global model,  
18  
19 324 using estuarine deposits (i.e. mouth terraces) together with barnacles, bryozoans and encrusting  
20  
21 325 foraminifera, for the period comprised between c. 5300 and 7000 cal. yr BP (Milne and Mitrovica,  
22  
23 326 2008).

24  
25  
26  
27 327 Regional considerations indicating that the existence of different rates of relative sea-level falls in  
28  
29 328 different sectors of Atlantic Patagonia, as reported in the past by Codignotto et al. (1992) and  
30  
31 329 refuted by recent works (Schellmann and Radke, 2010), need to be reconsidered. In this framework,  
32  
33 330 the existence of general tectonic components of uplift due to the subduction of the Nazca and the  
34  
35 331 Antarctic plates (Pedoja et al., 2011; Isla and Angulo, 2015) needs to be better clarified. Indeed, it is  
36  
37 332 necessary to identify the sectors characterized by different rates of uplift, by using a multi-indicator  
38  
39 333 approach and by searching further sea-level indicators, different from those traditionally used in this  
40  
41 334 area (Zanchetta et al., 2014). In this regard, it is fundamental to transform these indicators to sea-  
42  
43 335 level index points and to clarify the indicative meaning also of the previous indicators studied for  
44  
45 336 more correct regional correlations. This is particularly important for such a vast area, for which  
46  
47 337 good quality data are still sparse. An improvement in the quality of the indicators is a priority for  
48  
49 338 future research.

50  
51  
52  
53  
54 33955  
56  
57 340 **Acknowledgements**  
58  
59  
60



1  
2  
3 341 We thank J. Cause and the no-profit organization CADACE for the logistical support in the field  
4  
5 342 campaign. This work was funded by the University of Pisa (Progetto Ateneo 2007, Leader G.  
6  
7 343 Zanchetta, Progetto Ateneo 2014 Leader G. Zanchetta) and MIUR (PRIN2008, Leader G.  
8  
9 344 Zanchetta). We are strongly indebted to two anonymous reviewers for their insightful criticism and  
10  
11 345 encouraging suggestions that improved the manuscript.  
12  
13  
14 346

15  
16 347 **References**  
17  
18 348

- 19  
20 349 Alley RB, Clark PU, Huybrechts P, Joughin I (2005) Ice-Sheet and Sea-Level Changes. *Science*  
21 350 310: 456-460.  
22  
23 351  
24  
25 352 Angulo RJ, Giannini PCF, Suguio K, Pessenda LCR (1999) The relative sea-level changes in the  
26 353 last 5500 years southern Brazil (Laguna-Imbituba region, Santa Catarina State) based on vermetid  
27 354  $^{14}\text{C}$  ages. *Marine Geology* 159: 327–339.  
28  
29 355  
30 356 Angulo RJ., Lessa GC, de Souza MC (2006) A critical review of mid- to late-Holocene sea-level  
31  
32 357 fluctuations on the eastern Brazilian coastline. *Quaternary Science Reviews* 25: 486–506.  
33  
34 358  
35  
36 359 Bassi D, Iryu Y, Humblet M, Matsuda H, Machiyama H, Sasaki K, Matsuda S, Arai K, Inoue T  
37  
38 360 (2012) Recent macrofossils on the Kikai-jima shelf, Central Ryukyu Islands, Japan. *Sedimentology* 59:  
39 361 2024–2041.  
40  
41 362  
42  
43 363 Bini M, Isola I, Pappalardo M, Ribolini A, Favalli M, Ragaini L, Zanchetta G (2014)  
44  
45 364 Abrasive notches along the Atlantic patagonian coast and their potential use as sea level markers:  
46  
47 365 The case of Puerto Deseado (Santa Cruz, Argentina). *Earth Surface Processes and Landforms* 39:  
48  
49 366 1550-1558.  
50  
51  
52  
53  
54  
55  
56  
57  
58  
59  
60



- 1  
2  
3 368 Bini M, Consoloni I, Isola I, Pappalardo M, Ragaini L, Ribolini A, Zanchetta G (2013) Markers of  
4  
5 369 palaeo sea-level in rocky coasts of Patagonia (Argentina). *Rendiconti Online Societa Geologica*  
6  
7 370 *Italiana* 28: 24-27.  
8  
9 371  
10  
11 372 Baker RGV, Haworth RJ, Flood PG (2001) Warmer or cooler late Holocene marine  
12  
13 373 palaeoenvironments? Interpreting southeast Australian and Brazilian sea-level changes using fixed  
14  
15 374 biological indicators and their  $\delta^{18}\text{O}$  composition. *Palaeogeography, Palaeoclimatology,*  
16  
17 375 *Palaeoecology* 168:249-272.  
18  
19 376  
20  
21  
22 377 Blum MD and Roberts HH (2009) Drowning of the Mississippi Delta due to insufficient sediment  
23  
24 378 supply and global sea-level rise. *Nature geosciences* 2: 488-491.  
25  
26 379  
27  
28  
29 380 Butzin M, Prange B, Lohmann MG (2005) Radiocarbon simulations for the glacial ocean: The  
30  
31 381 effects of wind stress, Southern Ocean sea ice and Heinrich events. *Earth Planetary Science Letters*  
32  
33 382 235: 45-61.  
34  
35 383  
36  
37  
38 384 Clark JA, Farrell WF, Peltier WR (1978) Global Changes in Postglacial Sea Level: A Numerical  
39  
40 385 Calculation. *Quaternary Research* 9: 265-287.  
41  
42 386  
43  
44  
45 387 Codignotto JO, Kokot RR, Marcomini SC (1992) Neotectonism and sea level changes in the coastal  
46  
47 388 zone of Argentina. *Journal of Coastal Research* 8: 125-133.  
48  
49 389  
50  
51  
52 390 Cordero RR, Panarello H, Lanellotti S, Favier Dubois CM (2003) Radiocarbon age offsets between  
53  
54 391 living organisms from the marine and continental reservoir in coastal localities of Patagonia.  
55  
56 392 *Radiocarbon* 45: 9-15.  
57  
58 393  
59  
60

- 1  
2  
3 394 Isla IF and Angulo RJ (2015) Tectonic Processes along the South America Coastline Derived from  
4  
5 395 Quaternary Marine Terraces. *Journal of Coastal Research* in press.  
6  
7 396  
8  
9 397 Isla FI and Bujalesky GG (2008). Coastal geology and morphology of Patagonia and the Fuegian  
10  
11 398 Archipelago. In: Rabassa J (ed.) The late Cenozic of Patagonia and Tierra del Fuego. *Developments*  
12  
13 399 *in Quaternary Science* 11: 227–240.  
14  
15  
16 400  
17  
18 401 Isola I, Bini M, Ribolini A, Pappalardo M, Consoloni I, Fucks E, Boretto G, Ragaini L, Zanchetta G  
19  
20 402 (2011) Geomorphologic Map of Northeastern Sector of San Jorge Gulf (Chubut, Argentina).  
21  
22 403 *Journal of Maps* 2011: 476-485.  
23  
24 404  
25  
26  
27 405 Ferranti L, Antonioli F, Mauz B, Amorosi A, Dai Pra G, Mastonuzzi G, Monaco C, Orrù PE,  
28  
29 406 Pappalardo M, Radke U, Renda P, Romano P, Sansò P, Verrubi V (2006) Markers of the last  
30  
31 407 interglacial sea-level high stand along the coast of Italy: tectonic implications. *Quaternary*  
32  
33 408 *International* 145: 30-54.  
34  
35  
36 409  
37  
38 410 Feruglio E (1950) *Descripción geológica de la Patagonia*. Dirección General de Y.P.F., Tomo 3,  
39  
40 411 74-197, Buenos Aires.  
41  
42 412  
43  
44  
45 413 Gischler E and Möder A (2009) Modern benthic foraminifera on Banco Chinchorro, Quintana Roo,  
46  
47 414 Mexico. *Facies* 55: 27–35.  
48  
49 415  
50  
51 416 Laborel J and Laborel-Deguen F (1994) Biological indicators of relative sea-level variations and of  
52  
53 417 co-seismic displacement in the Mediterranean region. *Journal of Coastal Research* 395-415.  
54  
55  
56 418  
57  
58  
59  
60

- 1  
2  
3 419 Lema H, Busteros A, Franchi M (2001) Hoja Geológica 4566-II y IV, Camarones (1:250.000).  
4  
5 420 Programa Nacional de Cartas Geológicas de la República Argentina. Boletín N° 261, Buenos Aires,  
6  
7 421 53.  
8  
9 422  
10  
11 423 Lambeck K, Rouby H, Purcell A, Sun Y, Sambridge M. (2014) Sea level and global ice volumes  
12  
13 424 from the last glacial maximum to the Holocene. *PNAS* 111, 15296-15303.  
14  
15 425  
16  
17 426 López DA, Castro JM, González ML, Simpfendorfer RW (2003) Physiological responses to  
18  
19 427 hypoxia and anoxia in the giant barnacle, *Austromegabalanus psittacus* (Molina, 1782).  
20  
21 428 *Crustaceana* 76: 533-545.  
22  
23 429  
24  
25 430 López DA, Lopez BA, Pham CK, Isidro EJ, De Girolamo M (2010) Barnacle culture: background,  
26  
27 431 potential and challenger. *Aquaculture research* 41: 367- 375.  
28  
29 432  
30  
31 433 Martínez OA and Coronato AMJ (2008) The Late Cenozoic Fluvial Deposits of Argentine  
32  
33 434 Patagonia. In: J. Rabassa. The late Cenozoic of Patagonia and Tierra del Fuego. *Developments in*  
34  
35 435 *Quaternary Science* 11, 205-226.  
36  
37 436  
38  
39 437 Milne GA and Mitrovica JX (2008) Searching for eustasy in deglacial sea-level histories.  
40  
41 438 *Quaternary Science Reviews* 27: 2292–2302.  
42  
43 439  
44  
45 440 Milne GA, Gehrels WR, Hughes CW, Tamisiea ME, (2009) Identifying the causes of sea-level  
46  
47 441 change. *Nature Geoscience* 2: 471-478.  
48  
49 442  
50  
51 443 Milne GA, Long AJ, Bassett SE (2005) Modelling Holocene relative sea-level observations from  
52  
53 444 the Caribbean and South America. *Quaternary Science Reviews* 24: 1183-1202.  
54  
55  
56  
57  
58  
59  
60

- 1  
2  
3 445  
4  
5 446 PALSEA (PALeo SEA level working group) (2009) The sea-level conundrum: case studies from  
6  
7 447 palaeo-archives. *Journal of Quaternary Science* 25: 19–25.  
8  
9 448  
10  
11 449 Pappalardo M, Aguirre M, Bini M, Consoloni I, Fucks E, Hellstrom JC, Isola I, Ribolini A,  
12  
13 450 Zanchetta G (2015) Coastal landscape evolution and sea-level change: a case study from Central  
14  
15 451 Patagonia (Argentina). *Z. Geomorph.* 52: 145-172.  
16  
17 452  
18  
19  
20 453 Pavlis NK, Holmes SA, Kenyon SC, Factor JK (2012) The development and the evaluation of the  
21  
22 454 Earth gravitational model 2008 (EGM2008). *J. Geophys. Res. Solid Earth* 117: B04406.  
23  
24 455  
25  
26  
27 456 Pedoja K, Regard V, Husson L, Martinod J, Guillaume B, Fucks E, Iglesias M, Weill P (2011)  
28  
29 457 Uplift of quaternary shorelines in eastern Patagonia: Darwin revisited. *Geomorphology* 127: 121-  
30  
31 458 142.  
32  
33  
34 459  
35  
36 460 Perry CT and Hepburn LJ (2008) Syn-depositional alteration of coral reef framework through  
37  
38 461 bioerosion, encrustation and cementation: taphonomic signatures of reef accretion and reef  
39  
40 462 depositional events. *Earth-Science Review* 86: 106–144.  
41  
42 463  
43  
44 464 Pirazzoli PA, Delibrias G, Kawana T, Yanaguchi T (1985) The use of Barnacles to measure and  
45  
46 465 date relative sea-level changes in the Ryukyu Island, Japan. *Palaeogeography, Palaeoclimatology,*  
47  
48 466 *Palaeoecology* 49: 161-174.  
49  
50 467  
51  
52  
53 468 Ramos VA and Ghiglione MC (2008) Tectonic evolution of the Patagonian Andes. In: Rabassa J  
54  
55 469 (ed.) The late Cenozoic of Patagonia and Tierra del Fuego. *Developments in Quaternary Science,*  
56  
57 470 11: 57–71.  
58  
59  
60

- 1  
2  
3 471  
4  
5 472 Rasser M and Piller WE (1997) Depth distribution of calcareous encrusting associations in the  
6  
7 473 northern Red Sea and their geological implications. *Proc. 8<sup>th</sup> Int. Coral. Reef Symp.* 1: 743–748.  
8  
9 474  
10  
11 475 Reimer PJ, Bard E, Bayliss A, Beck JW, Blackwell PG, Bronk Ramsey C, Buck CE, Cheng H,  
12  
13 476 Edwards RL, Friedrich M, Grootes PM, Guilderson TP, Hafliðason H, Hajdas I, Hata C, Heaton  
14  
15 477 TJ, Hogg AG, Hughen KA, Kaiser KF, Kromer B, Manning SW, Niu M, Reimer RW, Richards  
16  
17 478 DA, Scott EM, Southon JR, Turney CSM, van der Plicht J (2015) IntCal13 and MARINE13  
18  
19 479 radiocarbon age calibration curves 0-50000 years cal BP. *Radiocarbon* 55(4). DOI:  
20  
21 480 10.2458/azu\_js\_rc.55.16947.  
22  
23 481  
24  
25 482 Ribolini A, Aguirre M, Baneschi I, Consoloni I, Fuck E, Isola I, Mazzarini F, Pappalardo M,  
26  
27 483 Zanchetta G, Bini M (2011) Holocene Beach Ridges and Coastal Evolution in the Cabo Raso Bay  
28  
29 484 (Atlantic Patagonian Coast, Argentina). *Journal of Coastal Research* 27: 973-983.  
30  
31  
32 485  
33  
34 486 Rostami K, Peltier WR, Mangini A (2000) Quaternary marine terraces, sea-level changes and uplift  
35  
36 487 history of Patagonia, Argentina: comparisons with predictions of the ICE-4G (VM2) model of the  
37  
38 488 global process of glacial isostatic adjustment. *Quaternary Science Reviews* 19: 1495-1525.  
39  
40  
41 489  
42  
43 490 Rovere A, Antonioli F, Bianchi CN (2015) Fixed Biological Indicators. In: Shennan I., Long AJ,  
44  
45 491 Horton BP (eds), *Handbook of Sea Level Research*. Wiley, pp. 268-280.  
46  
47  
48 492  
49  
50 493 Rovere A., Raymo ME, Vacchi M., Lorcheid T, Stocchi P., Gómez-Pujol L, Harris DL, Casella E,  
51  
52 494 O’Leary MJ, Hearty PJ (2016) The analysis of Last Interglacial (MIS5e) relative sea-level  
53  
54 495 indicators: Reconstructing sea-level in a warmer world, *Earth-Science Reviews* 159: 404-427.  
55  
56  
57 496  
58  
59  
60

- 1  
2  
3 497 Rutter N, Radtke U, Schnack EJ (1990) Comparison of ESR and amino acid data in correlating and  
4  
5 498 dating Quaternary shorelines along the Patagonian Coast, Argentina. *Journal of Coastal Research*  
6  
7 499 6: 391–411.  
8  
9 500  
10  
11 501 Rutter N, Schnack EJ, del Rio J et al. (1989) Correlation and dating of Quaternary littoral zones  
12  
13 502 along the Patagonian coast, Argentina. *Quaternary Science Reviews* 8: 213-234.  
14  
15 503  
16  
17  
18 504 Schellmann G and Radtke U (2000) ESR dating stratigraphically well-constrained marine terraces  
19  
20 505 along the Patagonian Atlantic coast (Argentina). *Quaternary International* 68/71: 261-273.  
21  
22 506  
23  
24  
25 507 Schellmann G and Radtke U (2003) Coastal terraces and Holocene sea-level changes along the  
26  
27 508 Patagonian Atlantic coast. *Journal of Coastal Research* 19: 963-996.  
28  
29 509  
30  
31  
32 510 Schellmann G and Radtke U (2010) Timing and magnitude of Holocene sea-level changes along the  
33  
34 511 middle and south Patagonian Atlantic coast derived from beach ridge systems, littoral terraces and  
35  
36 512 valley-mouth terraces. *Earth-Science Reviews* 103: 1–30.  
37  
38 513  
39  
40 514 Shennan I, Long AJ, Horton BP (2015) *Handbook of Sea-Level Research*. John Wiley & Sons, 634  
41  
42 515 pp.  
43  
44 516  
45  
46  
47 517 Shennan I and Horton BP (2002) Holocene land- and sea-level changes in Great Britain. *Journal of*  
48  
49 518 *Quaternary Science* 17: 511-526.  
50  
51 519  
52  
53  
54 520 Tamura T (2012) Beaches ridges and prograded beach deposits as paleoenvironmental records.  
55  
56 521 *Earth-Science Reviews* 114: 279-297.  
57  
58 522  
59  
60

- 1  
2  
3 523 Tanner WF (1995) Origin of beach ridges and swales. *Marine Geology* 129: 149-161.  
4  
5 524  
6  
7 525 Terrasi F, De Cesare N, D'Onofrio A, Lubritto C, Marzaioli F, Passariello I, Rogalla D, Sabbarese  
8  
9 526 C, Borriello G, Casa C, Palmieri A (2008) High precision  $^{14}\text{C}$  AMS at CIRCE. *Nuclear Instruments*  
10  
11 527 *and Methods in Physics Research* 266: 2221–2224.  
12  
13 528  
14  
15  
16 529 Terrasi F, Rogalla D, De Cesare N, D'Onofrio A, Lubritto C, Marzaioli F, Passariello I, Sabbarese  
17  
18 530 C, Casa G, Calmieri A, Gialanella L, Imbriani G, Roca V, Romano M, Sundquist M, Loger R  
19  
20 531 (2007) A new AMS facility in Caserta/Italy. *Nucl. Instr. Meth. Phys. Res., B* 259: 14-17.  
21  
22 532  
23  
24  
25 533 Vacchi M, Marriner N., Morhange C, Spada G, Fontana A, Rovere A. (2016) Multiproxy  
26  
27 534 assessment of Holocene relative sea-level changes in the western Mediterranean: Sea-level  
28  
29 535 variability and improvements in the definition of the isostatic signal. *Earth-Science Reviews*, 155:  
30  
31 536 172-197.  
32  
33  
34 537  
35  
36 538 Walker SE, Parsons-Hubbard K, Richardson-White S, Brett C, Powell E (2011) Alpha and beta  
37  
38 539 diversity of encrusting foraminifera that recruit to long-term experiments along a carbonate  
39  
40 540 platform-to-slope gradient: Paleocological and paleoenvironmental implications.  
41  
42 541 *Palaeogeography, Palaeoclimatology, Palaeoecology* 312: 305-324.  
43  
44 542  
45  
46  
47 543 Zanchetta G, Consoloni I, Isola I. et al. (2012) New insight on the Holocene marine transgression in  
48  
49 544 the Bahia Camarones (Chubut, Argentina). *Italian Journal of Geosciences* 131: 19–31.  
50  
51 545  
52  
53  
54 546 Zanchetta G, Bini M, Isola I, Pappalardo M, Ribolini A, Consoloni I, Boretto G, Fucks E, Ragaini  
55  
56 547 L, Terrasi F (2014) Middle-to late-Holocene relative sea-level changes at Puerto Deseado  
57  
58 548 (Patagonia, Argentina). *The Holocene* 24: 307-317.  
59  
60

1  
2  
3 Figure 1 -Location map of the studied area. Green circles: sites mentioned along the text; orange  
4 circle: location of Puerto Santa Elena; red square: study area; red stars: location of sampled sites.  
5  
6

7  
8 Figure 2 – Tide level derived from the current tide tables of Puerto Santa Elena. Elevation data are  
9 referred to the reduction plane (theoretical plane located under the mean sea level in order to have  
10 only positive tidal values in the tables). MLLW: Mean Lower Low Water; MLHW: Mean Lower  
11 High Water; MHLW: Mean Higher Low Water; MHHW: Mean Higher High Water; MHW: Mean  
12 High Water; MTL: Mean Tide Level.  
13  
14  
15  
16

17  
18 Figure 3 - Simplified geomorphological map of the studied area: H=Holocene beach ridges  
19 subdivided into H1, H2, H3 from the oldest to the youngest Beach Ridge, according to the  
20 morphostratigraphic units identified by Schellmann and Radke 2010; P= Pleistocene beach ridge.  
21  
22  
23

24  
25 Figure 4 - Geological sections (see map in Fig.2 for location): 2a) geological section AA'2b)  
26 geological section BB'; 2c) geological section CC'.  
27  
28

29  
30 Figure 5 - Elevation range of barnacles and incrustations in the three outcrops described. The data  
31 were measured by DGPS Trimble with a maximum error of 10 cm in elevation.  
32  
33

34  
35 Figure 6 - Images of barnacles (*Austromegabalanuspsittacus*) (a); incrustation (b); storm deposit  
36 infilling fractures within bedrock (c). Thin-section microscope photographs of the studied  
37 bioencrustations. A-B, encrusting acervulind shells (ac) showing chamber arrangement (arrows)  
38 with successive layers in sub-axial sections; the chambers are open in lateral walls (arrows). C,  
39 encrusting coralline algal thallus (cor) showing the transversal section of a uniporate conceptacle (c)  
40 with a cylindrical porecanal (arrow). Scale bar represents 500  $\mu$ m.  
41  
42  
43  
44  
45

46  
47 Figure 7 –Total plot of the Camarones area index points: fixed biological indicators from this work;  
48 valley mouth terrace indicators from Schellmann and Radke (2010). Limiting point from this work.  
49  
50

51  
52 Figure 8 – Relative sea level data (RSL) along the Patagonian coast for the “high stand” by different  
53 authors: redline: data from Codignotto et al. (1992); dark line: data from Zanchetta et al. (2014),  
54 and from this work reported as a.s.l.; (for sites location see fig.1 ). The indicative meaning reported  
55 in the figure is discussed in the text, while the indicative meaning cannot be reported for Codignotto  
56 et al. 1992.  
57  
58  
59  
60



1  
2  
3 Table 1 - Radiocarbon ages obtained for this study were performed using IntCal13 and MARINE13  
4 radiocarbon age calibration curves (Reimer et al. 2015). \*Data from Schellmann and Radke (2010)  
5  
6  
7  
8  
9  
10  
11  
12  
13  
14  
15  
16  
17  
18  
19  
20  
21  
22  
23  
24  
25  
26  
27  
28  
29  
30  
31  
32  
33  
34  
35  
36  
37  
38  
39  
40  
41  
42  
43  
44  
45  
46  
47  
48  
49  
50  
51  
52  
53  
54  
55  
56  
57  
58  
59  
60

For Peer Review

Lab. Code	Sample code	<sup>14</sup> C yr BP	Cal yr BP (±2σ)	Material	Elevation (m asl)
DSH2744	Wpi-424-2	5641±46	5924-6168	<i>Australomegabalanus psittacus</i>	3.7
DSH3170	Wpi-436A	5515±50	5741-6015	<i>Australomegabalanus psittacus</i>	3.6
DSH2738	AO-164	5132±67	5313-5608	<i>Australomegabalanus psittacus</i>	3.9
DSH2742	Wpi-436b	4995±89	5106-5560	Encrustation	3.6
DSH2736	AO-154D	5567±44	5865-6099	<i>Mytilus edulis</i>	3.9
DSH2745	Wpi-436	5562±43	5861-6092	<i>Mytilus edulis</i>	5.2
DSH4023	AO-164	5370±60	5604-5878	<i>Mytilus edulis</i>	3.5
Hd-23504	Pa04/7*	5560±38	5866-6065	<i>Protothaca antiqua</i>	3.8

For Peer Review

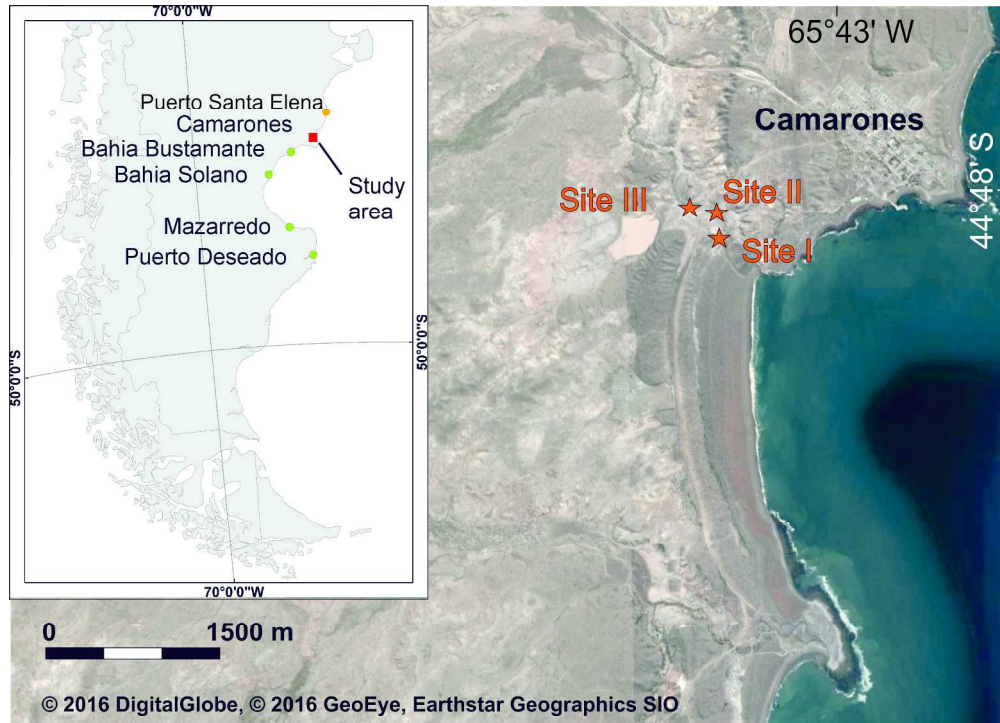


Figure 1 -Location map of the studied area. Green circles: sites mentioned along the text; orange circle: location of Puerto Santa Elena; red square: study area; red stars: location of sampled sites.

270x195mm (300 x 300 DPI)

review

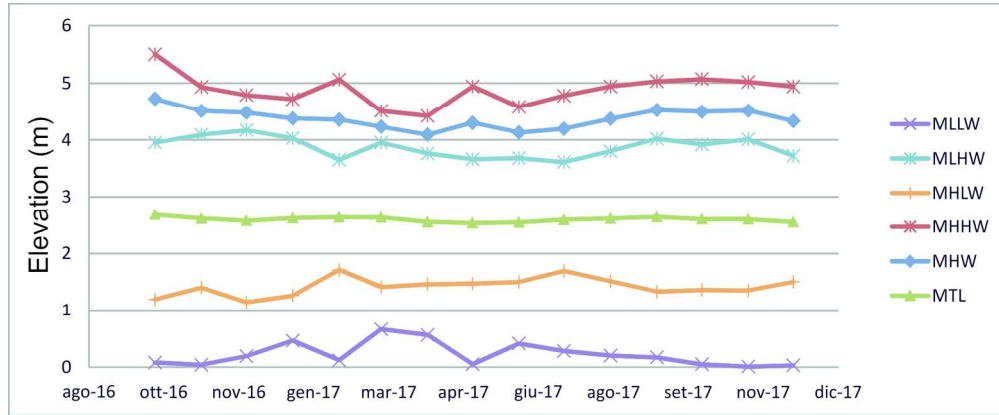


Figure 2 – Tide level derived from the current tide tables of Puerto Santa Elena. Elevation data are referred to the reduction plane (theoretical plane located under the mean sea level in order to have only positive tidal values in the tables). MLLW: Mean Lower Low Water; MLHW: Mean Lower High Water; MHLW: Mean Higher Low Water; MHHW: Mean Higher High Water; MHW: Mean High Water; MTL: Mean Tide Level.

185x76mm (300 x 300 DPI)

Peer Review

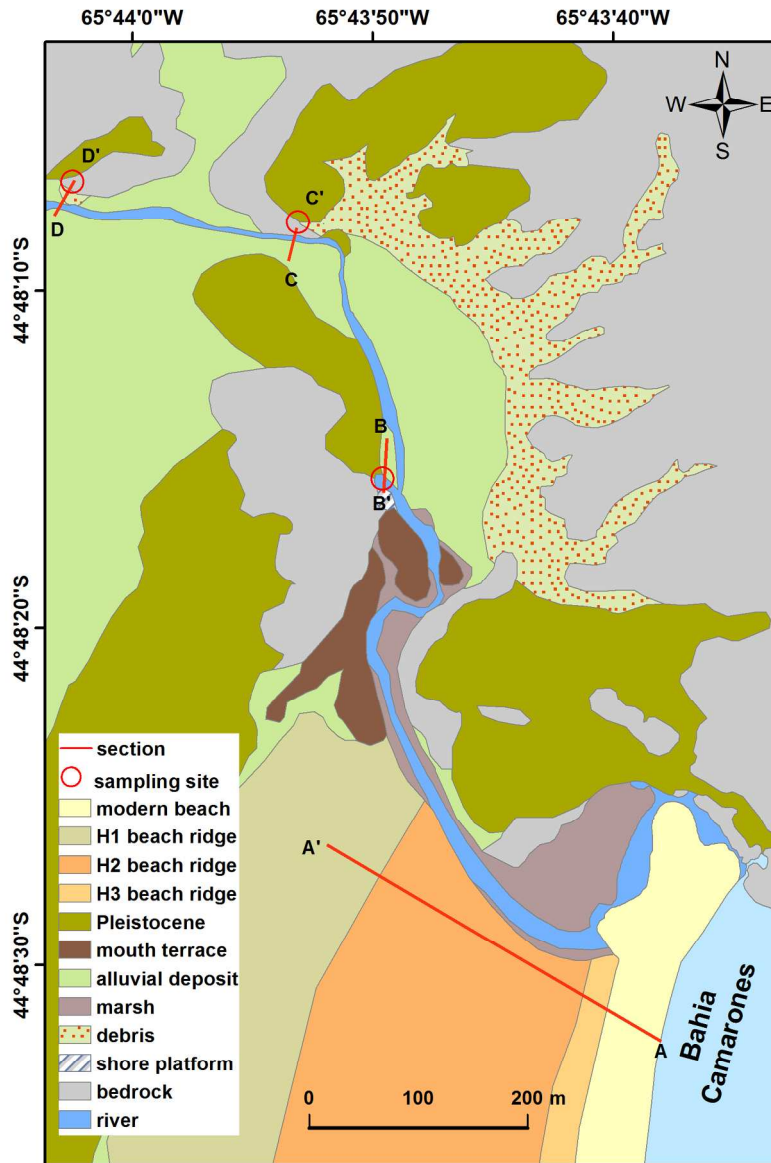


Figure 3 - Simplified geomorphological map of the studied area: H=Holocene beach ridges subdivided into H1, H2, H3 from the oldest to the youngest Beach Ridge, according to the morphostratigraphic units identified by Schellmann and Radke 2010; P= Pleistocene beach ridge.

150x219mm (300 x 300 DPI)

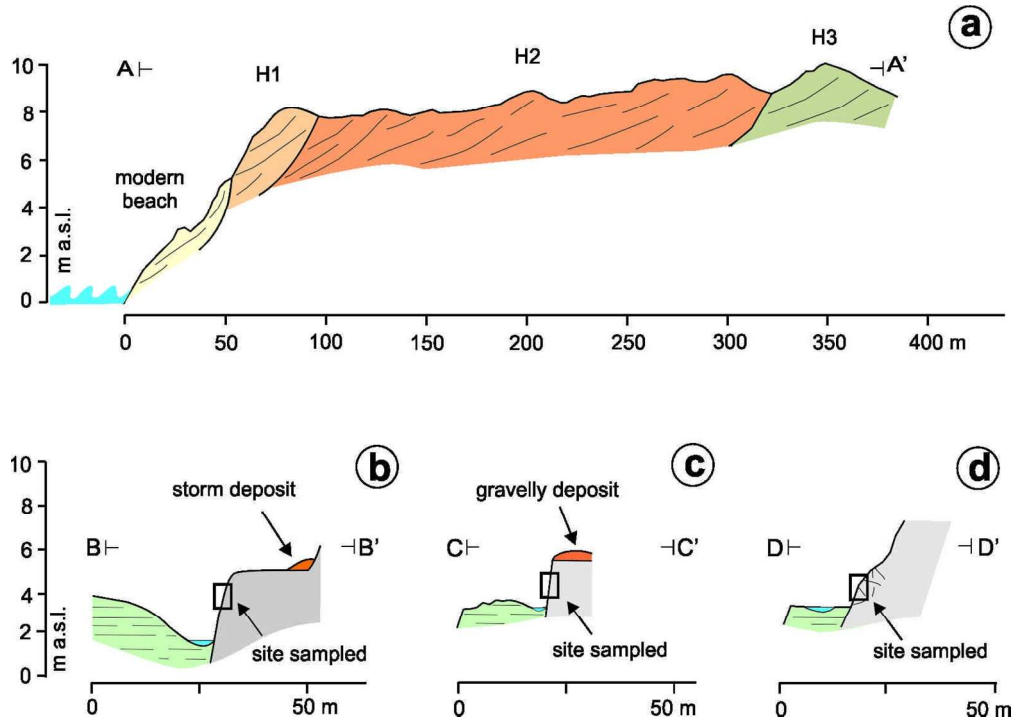


Figure 4 - Geological sections (see map in Fig. 3 for location): 2a) geological section AA'2b) geological section BB'; 2c) geological section CC'.

138x98mm (299 x 299 DPI)

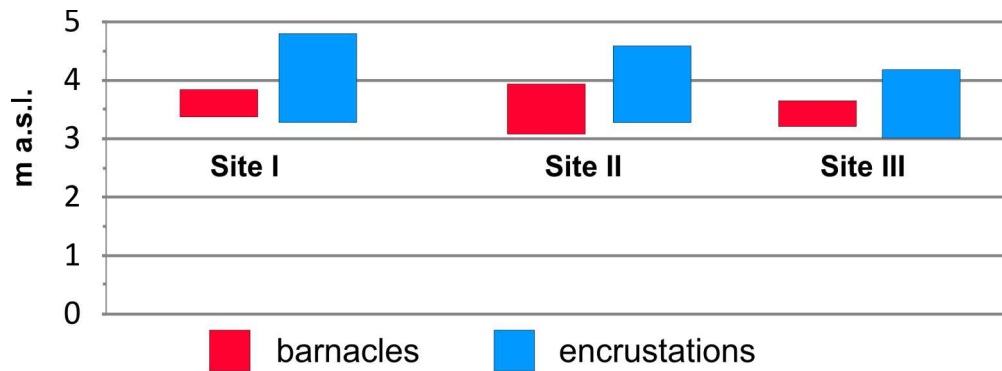
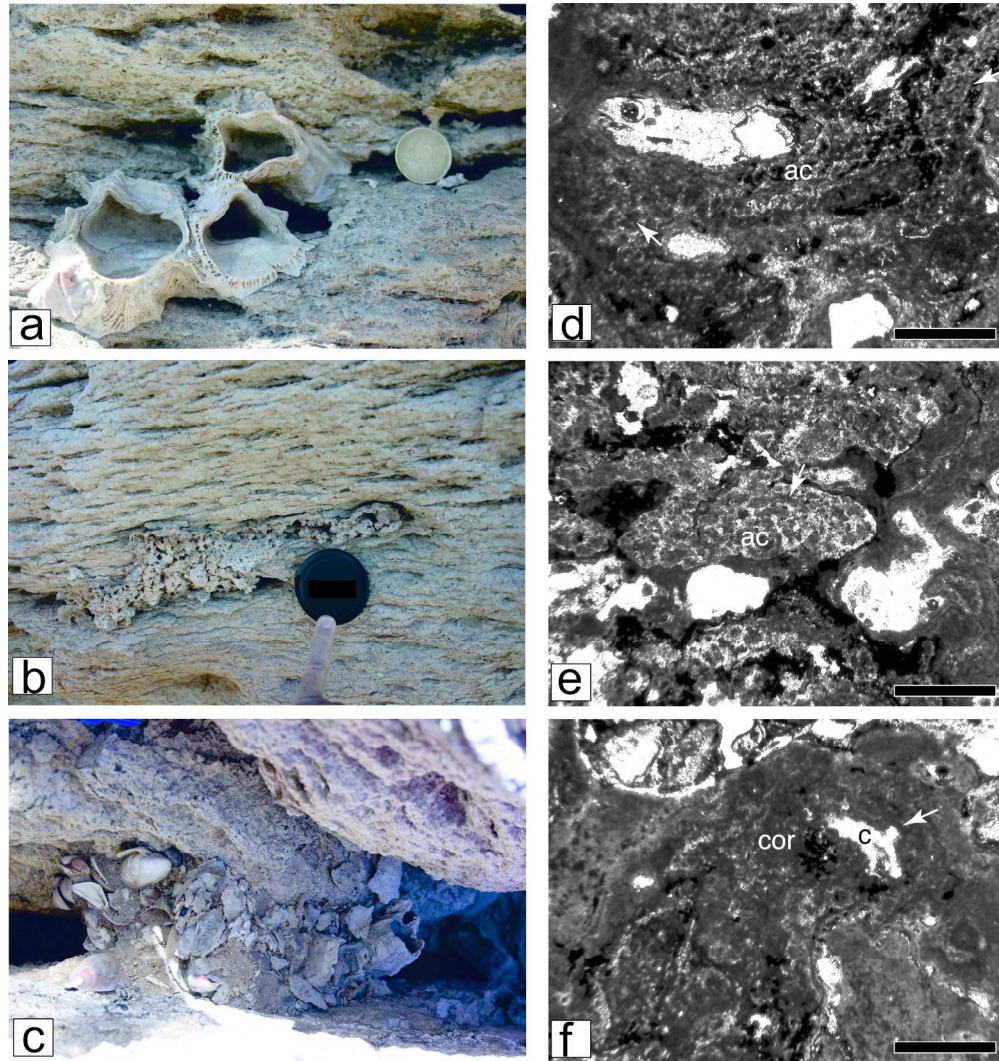


Figure 5 - Elevation range of barnacles and encrustations in the three outcrops described. The data were measured by DGPS Trimble with a maximum error of 10 cm in elevation.

170x61mm (300 x 300 DPI)





42  
43  
44  
45  
46  
47  
48  
49  
50  
51  
52  
53  
54  
55  
56  
57  
58  
59  
60

Figure 6 - Images of barnacles (*Austromegabalanuspsittacus*) (a); incrustation (b); storm deposit infilling fractures within bedrock (c). Thin-section microscope photographs of the studied bioencrustations. A-B, encrusting acervulind shells (ac) showing chamber arrangement (arrows) with successive layers in sub-axial sections; the chambers are open in lateral walls (arrows). C, encrusting coralline algal thallus (cor) showing the transversal section of a uniporate conceptacle (c) with a cylindrical pore canal (arrow). Scale bar represents 500  $\mu$ m.

182x193mm (300 x 300 DPI)



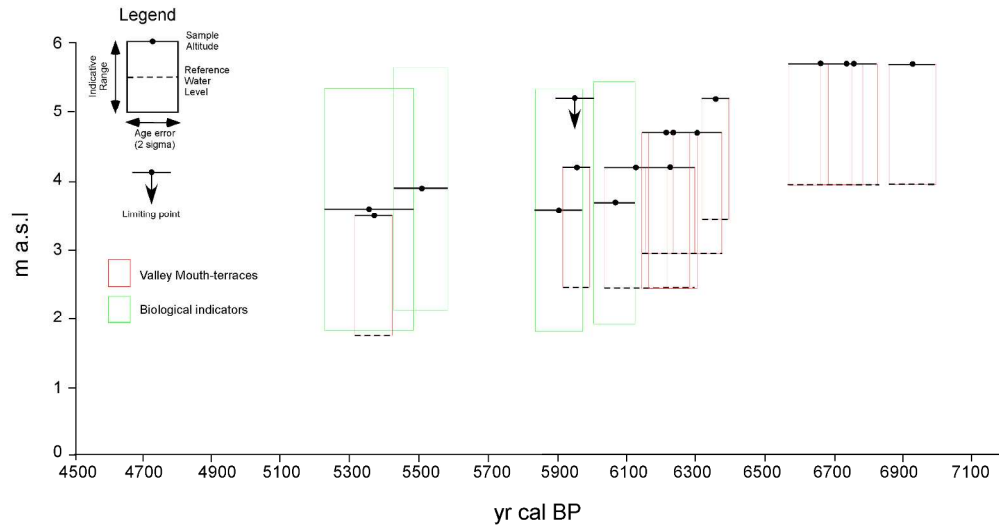


Figure 7 –Total plot of the Camarones area index points: fixed biological indicators from this work; valley mouth terrace indicators from Schellmann and Radke (2010). Limiting point from this work.

288x149mm (300 x 300 DPI)

Peer Review

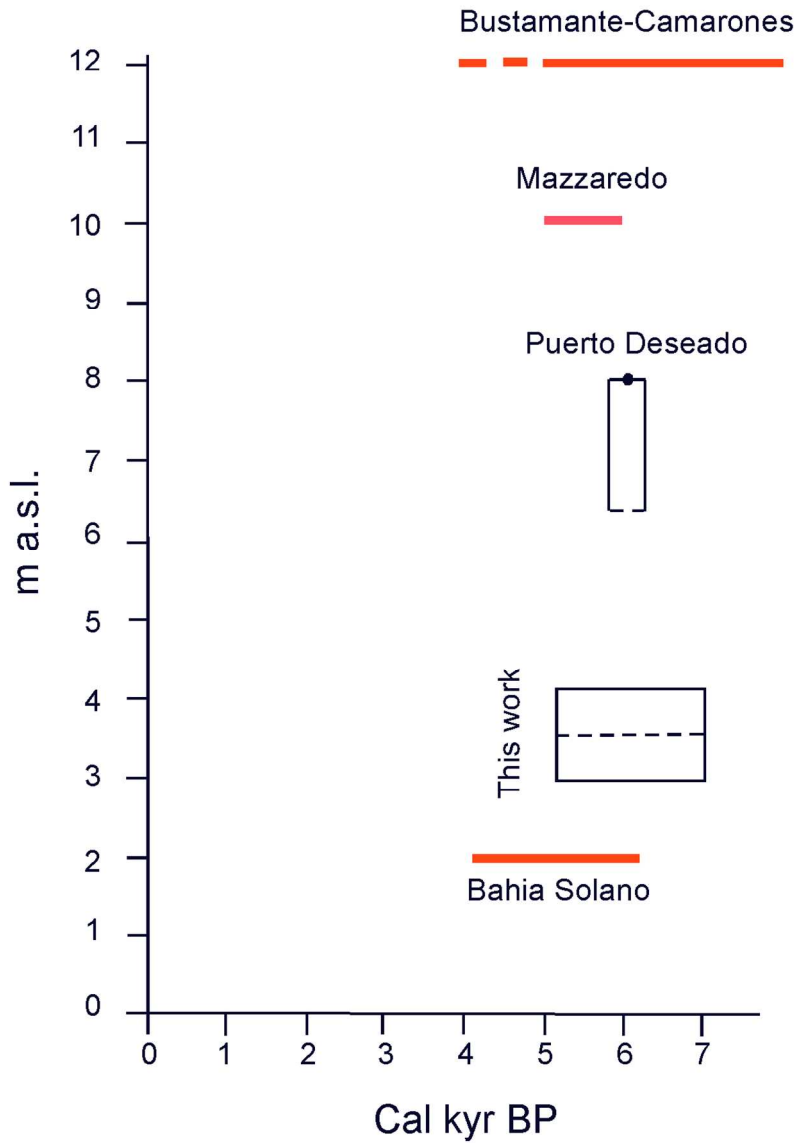


Figure 8 – Relative sea level data (RSL) along the Patagonian coast for the “high stand” by different authors: redline: data from Codignotto et al. (1992); dark line: data from Zanchetta et al. (2014), and from this work reported as a.s.l.; (for sites location see fig.1 ). The indicative meaning reported in the figure is discussed in the text, while the indicative meaning cannot be reported for Codignotto et al. 1992.

102x151mm (300 x 300 DPI)